# An Ossified Meckel's Cartilage in Two Cretaceous Mammals and Origin of the Mammalian Middle Ear

Yuanqing Wang, *et al.*

*Science* **294**, 357 (2001);
DOI: 10.1126/science.1063830

13. P. R. Cummins, B. L. N. Kennet, J. R. Bowman, M. G. Bostock, *Bull. Seismol. Soc. Am.* **82**, 323 (1992).
14. H. M. Benz, J. E. Vidale, *Nature* **365**, 147 (1993).
15. We included 1530 events with a depth from 0 to 75 km, a magnitude of $6.0 \leq M_w \leq 7.0$, and from stations in the epicentral distance range $100° \leq \Delta \leq 160°$ for the period 1 January 1980 to 29 March 1998. The SS phases in the individual traces are hand-picked, and the data is deconvolved for receiver effects and bandpass-filtered between 15 and 75 s.
16. The size of the caps corresponds to the Fresnel zone of the SS rays. Neighboring caps overlap partly to ensure smoothing.
17. B. Efron, R. Tibshirani, *Science* **253**, 390 (1991). The data set was also divided into two subsets with epicentral distances from 100° to 130° and 130° to 160°; splitting was still present in stacks of the subsets.
18. Supplementary material is available at www.sciencemag.org/cgi/content/full/294/5541/354/DC1
19. The stacks are cross-correlated with the SS pulse; splitting is determined by two cross-correlation maxima (instead of one) in the depth range of 480 to 600 km.
20. We find single reflections from 520 km for stacks corresponding to different regional types (shields, tectonically active regions, stable continents, and oceans). The stacks exhibit somewhat different amplitudes and, in particular, the shield stack shows a smaller amplitude, confirming an earlier study (*6*).
21. N. A. Simmons, H. Gurrola, *Nature* **405**, 559 (2000).
22. D. Canil, *Phys. Earth Planet. Inter.* **86**, 25 (1994).
23. S. Koito, M. Akaogi, O. Kubuta, T. Suzuki, *Phys. Earth Planet. Inter.* **120**, 1 (2000).
24. D. J. Weidner, Y. Wang, in *Earth's Deep Interior: Mineral Physics and Tomography from the Atomic to the Global Scale* (Geophysical Monograph 117, American Geophysical Union, Washington, DC, 2000), pp. 215–235.
25. J. Ritsema, H. J. van Heijst, J. H. Woodhouse, *Science* **286**, 1925 (1999).
26. Y. Fei, C. Bertka, in *Mantle Petrology: Field Observations and High-Pressure Experimentation*, Special Publication in honor of Francis R. Boyd, *Geochem. Soc. Spec. Pub.* (Geochemical Society, Washington University, St. Louis, MO, 1999), vol. 6, pp. 189–207.
27. T. Inoue, D. J. Weidner, P. A. Northrup, J. B. Parise, *Earth Planet. Sci. Lett.* **160**, 107 (1998).
28. H. Yusa, T. Inoue, Y. Ohishi, *Geophys. Res. Lett.* **27**, 413 (2000).
29. A. Dziewonski, D. Anderson, *Phys. Earth Planet. Inter.* **25**, 297 (1981).
30. Previous SS-precursor studies suggest a shear wave impedance contrast of 6 to 10% for the 410-km discontinuity and 10% for the 660-km discontinuity (*9*). In the mid–transition zone region, computer simulations for a pyrolite mantle composition give a jump of 1.66% in shear wave impedance for the garnet transition and 3.13% for the olivine transition of the β-phase to γ-phase (*24*).
31. W. D. Mooney, G. Laske, G. Masters, *Eos (Fall Suppl.)* **76**, F421 (1995).
32. C. H. Chapman, *Geophys. Res. Lett.* **3**, 153 (1976). The synthetics are basically delta pulses computed using WKBJ ray tracing for PREM (including attenuation from PREM) and then filtered in the same way as the data.
33. We thank A. Jephcoat and A. Kleppe for useful discussions on mineralogical phase transitions. A.D. was funded by a Scatcherd Scholarship from Oxford University. We also acknowledge support under U.K. Natural Environment Research Council grant GR11534.

18 June 2001; accepted 24 August 2001

# An Ossified Meckel's Cartilage in Two Cretaceous Mammals and Origin of the Mammalian Middle Ear

**Yuanqing Wang,[1]* Yaoming Hu,[1,2,3] Jin Meng,[2]* Chuankui Li[1]**

**An ossified Meckel's cartilage has been recovered from two early Cretaceous mammals from China. This element is similar to Meckel's cartilage in prenatal and some postnatal extant mammals and indicates the relationship of Meckel's cartilage with the middle ear in early mammals. The evidence shows that brain expansion may not be the initial factor that caused the separation of postdentary bones from the dentary as middle ear ossicles during mammalian evolution. The failure of the dentary to seize reduced postdentary elements during ontogeny of early mammals is postulated as an alternative mechanism for the separation. Modifications of both feeding and hearing apparatuses in early mammals may have led to the development of the definitive mammalian middle ear.**

In nonmammalian vertebrates with jaws, the craniomandibular joint is between the quadrate region of the palatoquadrate and the articular region of Meckel's cartilage (or its replacement). In unequivocal mammals (*1, 2*), the joint is between the squamosal and the dentary. The definitive mammalian middle ear (DMME) is formed by transference of accessory jaw elements, including the angular, articular plus prearticular, and quadrate, to the cranium of mammals as strictly auditory ossicles (renamed as the tympanic, malleus, and incus) (*3*). This transference is one of the central topics of comparative anatomy and evolutionary biology of vertebrates (*3–8*). Although developmental studies of extant mammals have long demonstrated homologies of these elements among jawed vertebrates (*9, 10*), the only fossil evidence on this critical transference is the presence of persistent grooves on the medial surface of the dentary bone, which may have lodged the anterior end of the postdentary unit (PDU, consisting of the endochondral articular and dermal prearticular, angular, and surangular) in some early mammals (*3*).

Four nearly complete *Repenomamus* adult skulls with articulated lower jaws (*11*) and one with articulated lower jaws of an unnamed *Gobiconodon* species (Figs. 1 and 2) were discovered from the Yixian Formation of the lower Cretaceous in Liaoning, China (*12*). Of the two taxa, *Repenomamus* (*11*) represents one of the largest Mesozoic mammals, and is most closely related to gobiconodontids (*13–15*) in sharing basic structures of jaws, teeth, occlusal pattern, and some cranial features (Figs. 1 to 3). Gobiconodontids are related to triconodontids within triconodonts, a diverse grade of basal mammaliaform groups with uncertain relationships (*2, 15–18*) (Fig. 3). Among these specimens, a structure that we recognize as an ossified Meckel's cartilage (OMC) was preserved in two skulls of *Repenomamus* (IVPP specimens V12549 and V12728) and one skull of *Gobiconodon* (IVPP V12585). Of the two OMCs in *Repenomamus*, the one in V12549 is in its original location (Figs. 1, A to C, and 2, A and C), whereas the other in V12728 is displaced and lies between the mandible and the skull (Figs. 1D and 2B). The OMC is rod-like, with a pointed anterior tip and a flared posterior end. It measures 33 mm long in V12549 and 40 mm in V12728. The anterior portion of the OMC in V12549 is lodged in a depression that appears to be an expanded posterior portion of the meckelian groove. The OMC-dentary contact may have had some mobility. During preparation, the OMC was separated from the dentary. In all lower jaws of *Repenomamus*, the anterior tip of the meckelian groove is below m3 (the third lower molariform tooth) and continues anteriorly as a slit that parallels the course of the mandibular canal within the dentary. The mandibular canal, as revealed by radiographic imaging, is low in position, ventral to the long roots of the check teeth, and extends anteriorly to the symphysis. The radiograph shows that in lateral view, the mandibular canal turns slightly dorsally at the position where the anterior tip of the OMC is situated, and extends posteriorly to the mandibular

[1]Institute of Vertebrate Paleontology and Paleoanthropology (IVPP), Chinese Academy of Sciences, Post Office Box 643, Beijing, 100044, China. [2]Division of Paleontology, American Museum of Natural History (AMNH), Central Park West at 79th Street, New York, NY 10024, USA. [3]Biology Program (Ecology, Evolutionary Biology, and Behavior), Graduate School and City College, City University of New York, NY 10016–4309, USA.

*To whom correspondence should be addressed. E-mail: wang.yuanqing@pa.ivpp.ac.cn (Y.W.); jmeng@amnh.org (J.M.)

foramen. Posterior to the mandibular foramen, the OMC curves medially to depart from the dentary. A flat facet is on the dorsal side of the free segment of the OMC (Fig. 1, F and G). The flared posterior end of the OMC lies ventral to the lateral flange of the petrosal at the basicranial region (Fig. 2). Rugosities on the posterior end of the OMC suggest that it was connected by ligament to the lateral flange during the mammal's lifetime. The OMC in *Gobiconodon* sp. (V12585; Fig. 1E) is proportionally thicker than those of *Repenomamus*. Its posterior end is broken, whereas the anterior end is still at the meckelian groove (Fig. 1E).

The OMC in *Repenomamus* was originally identified as the "postdentary bar" (*11*). In the mandible of close relatives of mammals, two sets of accessory elements are attached to the dentary. These are the paradentary bones (the coronoid and splenial) and the postdentary bones (those constituting the PDU) (*3, 5*). The paradentary bones are platelike and have no relationship with the basicranium (*3, 5, 19*). Within the PDU, the articular has a retroarticular process and extends posteriorly to articulate with the quadrate. The surangular also extends posteriorly to articulate either with the squamosal or with the quadrate (*3, 5, 19*). The angular bears a reflected lamina and is complex in shape. The prearticular in *Morganucodon* is straight and posteriorly fused to the articular. Given that all other accessory bones in *Repenomamus* are detached from the dentary and are small (estimated from the sizes of the fossa incudis and oval window, distance between these structures, and the general size of the ear region), the bone in question is too big to be a prearticular. A hyoid element is also preserved in V12728 and is much smaller than the OMC (Fig. 1H). The hyoid elements form a chain of ossicles from the ear region to the larynx in mammals; none of them is lodged in the dentary. Therefore, the shape and size of the bone in question and its relationship to the dentary and cranium indicates that it is not any of the accessory jaw bones or hyoid elements. The bone is most probably the ossified middle portion of Meckel's cartilage. Its shape and relation to the cranium and dentary are closely similar to those of Meckel's cartilage of prenatal and some postnatal extant mammals (*6, 8, 20–22*). Even in fully grown juveniles of living mammals, Meckel's cartilage can still exist between the dentary and ear region (*23*). Persistence of Meckel's cartilage in adults of the common ancestor of mammals has been inferred (*8, 16*), although there is no direct evidence.

Developmental studies of living mammals have revealed that the posterior end of Meckel's cartilage forms the anlage of the malleus and that the middle portion of the cartilage degenerates in the later stages of ontogeny. Its sheath becomes the spheno-

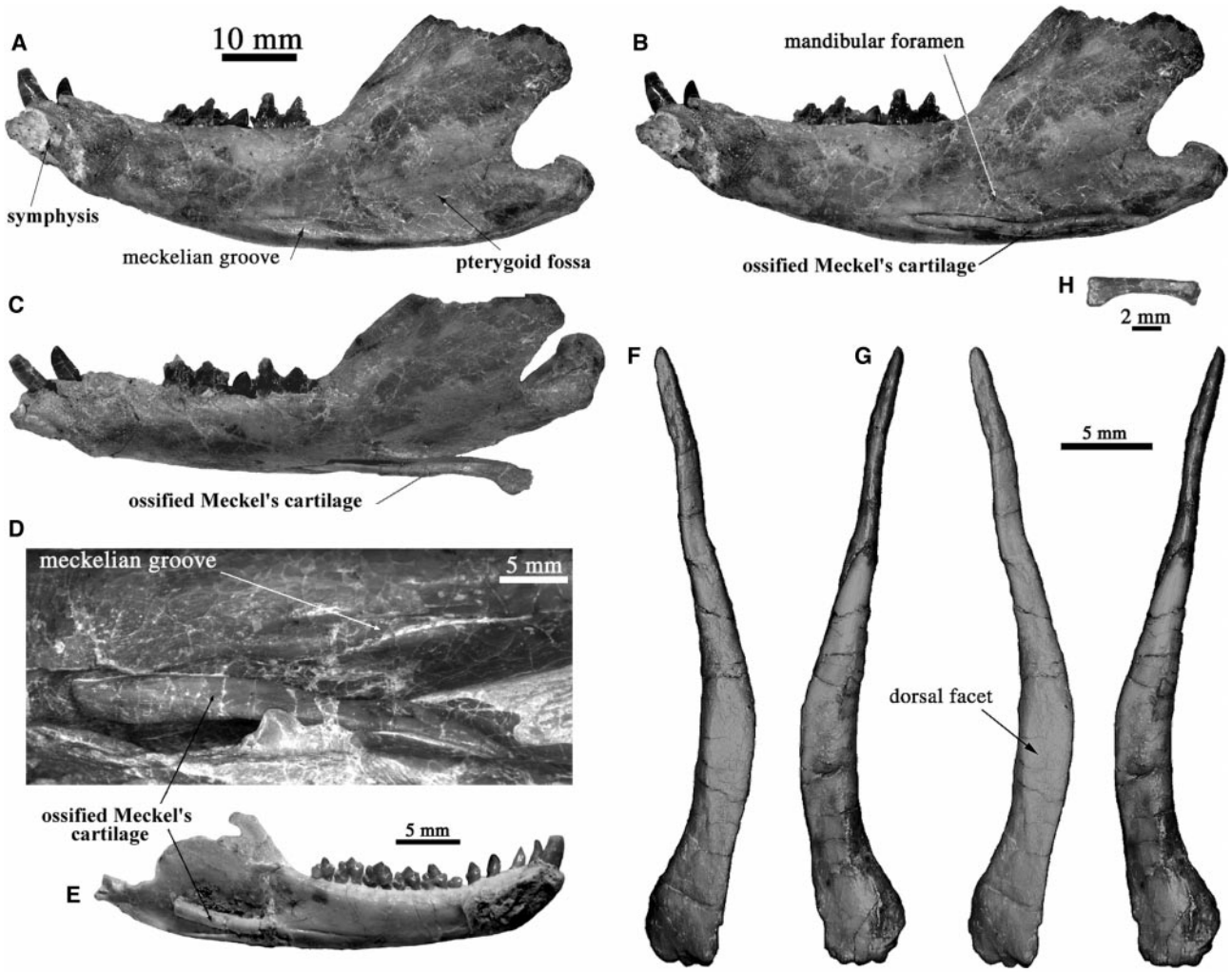


**Fig. 1.** Mandibles and the ossified Meckel's cartilage (OMC) of *Repenomamus* and *Gobiconodon* sp. (**A** and **B**) Medial views of the right mandible of *Repenomamus* (IVPP specimen V12549) with the OMC being removed in (A). (**C**) Dorsomedial view of V12549 with the OMC attached. (**D**) Ventromedial view of a *Repenomamus* skull (V12728) showing the right OMC and meckelian groove (see also Fig. 2B). (**E**) Medial view of the left mandible with the attached OMC in *Gobiconodon* sp. (V12585.2). (**F** and **G**) Stereophotographs of dorsal (F) and ventral (G) views of the OMC in V12549. (**H**) A hyoid element from V12728. Additional morphologic data can be found in supplementary data (*34*).

mandibular ligament (pterygomandibular in monotremes) and the anterior ligament of the malleus (*3, 9, 10*). The OMC in *Repenomamus* and *Gobiconodon* provides evidence for the relationship of Meckel's cartilage with the DMME in early mammals, which is otherwise inferred only from embryological evidence of living mammals.

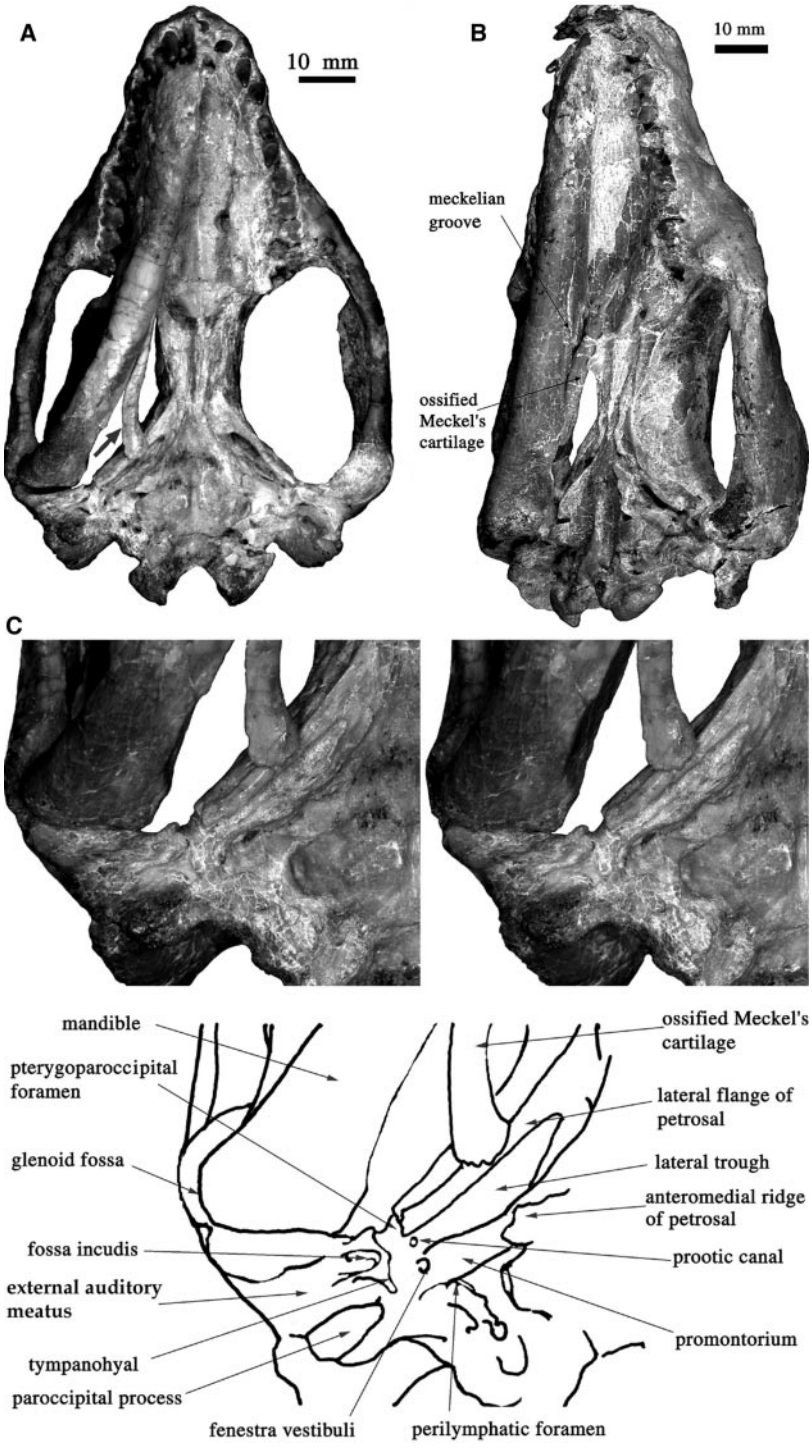


**Fig. 2.** Skulls and basicranial region of *Repenomamus*. (**A**) Ventral view of V12549, showing relationship of the ossified Meckel's cartilage (indicated by arrow) with the dentary and ear region. (**B**) Ventromedial view of V12728 showing the displaced OMC. (**C**) Close ventral view of the basicranial region (V12549). The maximum skull dimensions of V12549 are 108 mm by 71 mm. Using the method of (*18*), the width of the "brain vault" is 28 mm, which is the maximum distance between the squamosal-parietal sutures. The width between the temporomandibular joints is 60 mm (between the midpoints of the glenoid fossae). The actual brain vault of *Repenomamus* is narrower, as reviewed by radiographic imaging and by direct observation from a broken skull (V12613) in which the wall of the braincase measures 3.7 mm thick.

It also shows that, while the anlage of the malleus is reduced, or posteriorly shifted, to form the malleus, a significant middle segment of Meckel's cartilage is persisted and ossified in adults, probably remaining in its early ontogenetic position. A similar condition is probably present in other early mammals, such as triconodontids and symmetrodontids. The function of the OMC in adults of these mammals is unclear. A dorsal facet on the OMC of *Repenomamus* (Fig. 1F) suggests that muscle was attached. If so, the OMC may have functioned as the inflected angular process in marsupials (*24*), or the pterygoid shelf in multituberculates (*25*), for partial insertion of the medial pterygoid muscle that originates on the pterygoid region of the skull. When opening and closing the lower jaw, the attached OMC could rotate with the jaw, with its contact at the lateral flange serving as the fulcrum. Mastication may not have interfered with hearing in *Repenomamus*.

Identification of the OMC leads to the conclusion that *Repenomamus* and *Gobiconodon* have a DMME, because the dentary of the two taxa lacks other scars for the PDU. The fossa incudis immediately medial to the secondary craniomandibular joint (SCMJ, dentary-squamosal) in *Repenomamus* indicates an intermediate condition between the mandibular ear of nonmammalian synapsids, such as *Morganucodon*, and the DMME of more advanced mammals in which the ear ossicles are widely separated from the SCMJ and lie behind intervening secondary auditory structures (*7*). This relationship shows that in early mammals the SCMJ is lateral, not anterior [as shown in ontogenesis of living mammals (*8, 9*)], to the primary joint (malleo-incudal = quadrate-articular); the ear ossicles are medial, not posterior [as shown in extant mammals (*7*)], to the SCMJ. Other features of *Repenomamus*, such as an elongated promontorium and a distinct external auditory meatus, can be attributed to more efficient hearing of airborne sound, while the expanded glenoid fossa and mandibular condyle, enlarged pterygoid, and broad masseteric fossa (Figs. 1, A to E, and 2) are related to more powerful mastication.

Discovery of the OMC helps to interpret grooves present near the mandibular foramen of the dentary in many early mammals and their relatives. These puzzling grooves were known at least since Owen (*26*) and have been considered either as holding dental nerves and arteries (*13, 27*) or as facets for the PDU in *Peramus* and *Amphitherium* (*3*). Because *Peramus* and *Amphitherium* are in the Trechnotheria (*1*) (Fig. 3), the latter interpretation of the PDU in these taxa argues for multiple origins of the DMME (*3*). Our evidence demonstrates that in some early mammals, an OMC is probably the primary

occupant for the grooves in question. The evidence, viewed within the phylogeny, weakens the hypothesis of multiple origins of the DMME (*3*).

The phylogeny based on 112 craniodental characters from 20 taxa (Fig. 3) is largely in keeping with other recent phylogenetic hypotheses of mammals and their relatives (*2, 15–18*). Within the phylogeny, acquisition of the DMME in *Repenomamus* and *Gobiconodon* is consistent with the prediction that triconodontids have ear ossicles (*3*). Whether the DMME is a synapomorphy for Mammalia, which probably occurred in the middle Jurassic, or it is shared by Mammalia and *Hadrocodium* and thus evolved in the early Jurassic (*18*) (Fig. 3), depends on the interpretation of *Hadrocodium*. The type specimen of *Hadrocodium* (IVPP V8275) was originally regarded as a juvenile *Morganucodon* (*28*), but is now considered an adult, or subadult, of a distinctive taxon in which the PDU is detached from the dentary (*18*). In our view, however, many features, such as its small size, erupting first upper postcanine tooth (*28*), only two molars, slender mandible, large space between m2 and the coronoid process, large promontorium, and large brain vault (*18*), suggest that V8275 is a postsuckling juvenile. Whether the common ancestor of *Hadrocodium* and mammals evolved the DMME in the early Jurassic requires further testing (Fig. 3).

The most uncertain issue in the evolution of the DMME is how the PDU became detached from the dentary and translocated to the basicranium as ear ossicles (*3–8*). One model suggests that brain expansion increased the distance between the middle ear and the mandible during ontogeny and evolution of mammals and thus tore off the ear ossicles from the mandible (*7, 18*). This model is not consistent with the narrow braincases of our specimens of *Repenomamus* and *Gobiconodon*. The maximum ratio of the estimated brain vault to the skull width in V12549 of *Repenomamus* is 49% (see Fig. 2 caption), smaller than those of *Sinoconodon* and *Morganucodon*, in which the PDU is still attached to the dentary (*18, 29, 30*). This indicates that detachment of the ear ossicles is not necessarily associated with expansion of the brain during mammalian evolution. In *Repenomamus*, the fossa incudis, which reflects the position of the incus and malleus, is immediately medial to the SCMJ. The distance between the SCMJ and the fossa incudis is proportionally similar to, or even smaller than, the space between the quadrate recess and the SCMJ in *Morganucodon* (*18, 30, 31*). This shows that separation of the PDU from the dentary does not require greater distance between the ear and the mandible.

Our specimens permit an alternative hypothesis for the origin of the DMME. During evolution of synapsids, the PDU is reduced in size and loosened to enhance hearing of high-frequency airborne sounds (*5*), whereas the dentary was enlarged for attachment of more muscle to facilitate efficient mastication (*3, 32, 33*). The position of the OMC in *Repenomamus* suggests that the common ancestor of mammals probably had a developmental pattern in which Meckel's cartilage extended from dentary to the ear region. Because of its close relationship with the cartilage, the dentary was probably tilted in position. Reduction of the PDU increasingly weakened its tie to the dentary until a critical point was reached where the dentary, while erecting to a more vertical position during ontogeny, no longer seized the PDU, which was moored at the basicranium by connective tissue. This hypothesis is similar to the detaching mechanism of the ear ossicles in marsupials (*6*), without requiring brain expansion as the initial trigger. Modifications in both feeding and hearing apparatuses toward efficient functions have led to the decoupling of the PDU and dentary. Expansion of the brain, along with changes in the otic capsule, may have caused displacements of the ear ossicles to a position either more vertical (*6*), horizontal (*8*), or posteriorly distant from the SCMJ (*7*) in more advanced mammals.

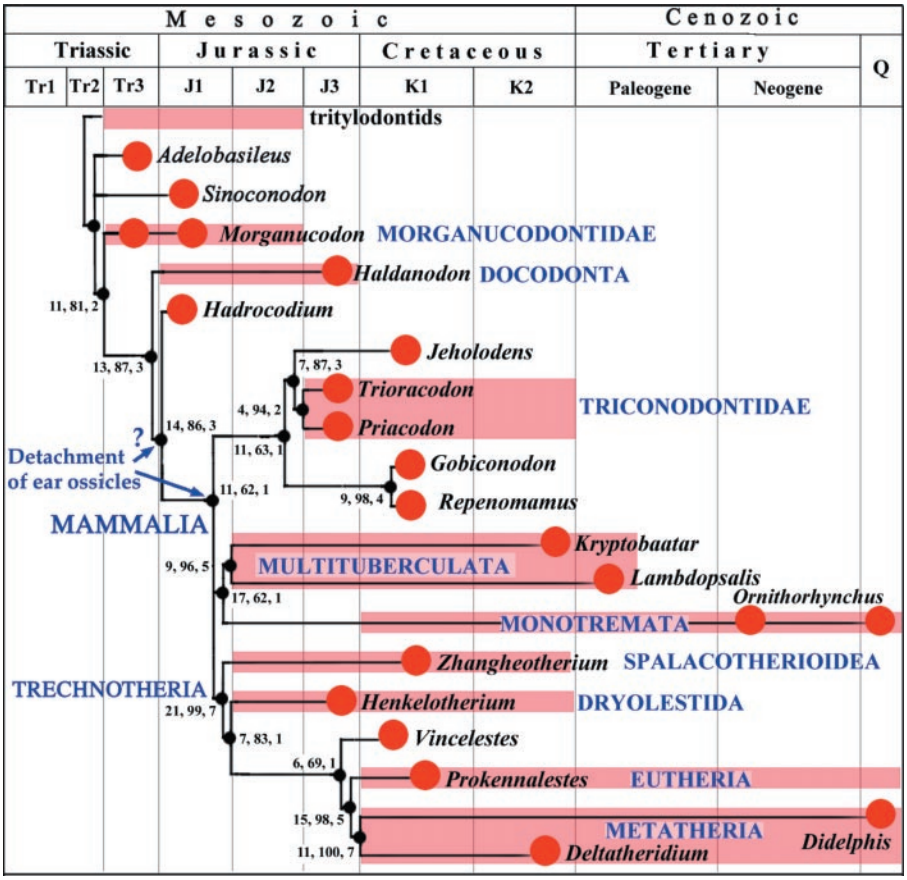


**Fig. 3.** Phylogenetic relationships and distributions of main mammaliaform groups. The cladogram is the consensus (tree length = 275; CI = 0.589; RI = 0.706) of four equally most-parsimonious trees that are obtained by branch-and-bound searches using PAUP* 4.0 b8 based on 112 craniodental characters across 20 terminal taxa. Search options include: all characters unordered, equally weighted, accelerated transformation, multistate as uncertainty, rooting at tritylodontids, and monophyletic in-group. Numbers at each node represent assigned branch length, bootstrapping value, and Bremer supporting index. Bootstrapping value is obtained by 1000 replications of heuristic searches. Red dots represent occurrences of genera (*1*) used in the phylogenetic analyses. Pink bars are distributions of higher taxa (*1*) represented by the genera. Character list, sources of data, and detailed tree descriptions can be found in supplementary data (*34*).

## References and Notes


1. M. C. McKenna, S. K. Bell, *Classification of Mammals Above the Species Level* (Columbia Univ. Press, New York, 1997).
2. T. Rowe, *J. Vertebr. Paleontol.* **8**, 241 (1988).
3. E. F. Allin, J. A. Hopson, in *The Evolutionary Biology of Hearing*, D. B. Webster, R. R. Fay, A. N. Popper, Eds. (Springer-Verlag, New York, 1992), pp. 587–614.
4. J. A. Hopson, *Am. Zool.* **6**, 437 (1966).
5. E. F. Allin, *J. Morphol.* **147**, 403 (1975).
6. W. Maier, *Neth. J. Zool.* **40**, 55(1990).
7. T. Rowe, *Mem. Cal. Acad. Sci.* **20**, 71 (1996).
8. U. Zeller, in *Mesozoic Differentiation, Multituberculates, Monotremes, Early Therians, and Marsupials*, vol. 1, *Mammal Phylogeny*, F. S. Szalay, M. J. Novacek, M. C. McKenna, Eds. (Springer-Verlag, New York, 1993), pp. 95–107.
9. E. Gaupp, *Die Reichertsche Theorie* (Archiv für Anatomie und Entwicklungsgeschichte, 1912, Hammer-, Amboss-, und Kieferfrage, 1913).

10. E. S. Goodrich, *Studies on the Structure and Development of Vertebrates* (Macmillan, London, 1930).
11. J.-l. Li, Y. Wang, Y.-q. Wang, C-k. Li, *Chin. Sci. Bull.* **45**, 2545 (2000).
12. X.-l. Wang *et al.*, *Vert. PalAsiat.* **36**, 81 (1998).
13. F. A. Jr. Jenkins, C. R. Schaff, *J. Vertebr. Paleontol.* **8**, 1 (1988).
14. Z. Kielan-Joworoska, D. Dashzeveg, *Acta Palaeontol. Pol.* **43**, 413 (1998); H.-J. Kuhn, *Abh. Senckenb. Naturforsch. Ges.* **28**, 1 (1971).
15. Q. Ji, Z.-x. Luo, S.-a. Ji, *Nature* **398**, 326 (1999).
16. G. W. Rougier, J. R. Wible, M. J. Novacek, *Am. Mus. Novit.* **3187**, 1 (1966).
17. Y.-m. Hu, Y.-q. Wang, Z.-x. Luo, C.-k. Li, *Nature* **390**, 137 (1997).
18. Z.-x. Luo, A. W. Crompton, A.-l. Sun, *Science* **292**, 1535 (2001).
19. K. A. Kermack, F. Mussett, H. W. Rigney, *Zool. J. Linn. Soc.* **53**, 87 (1973).
20. H.-J. Kuhn, *Abh. Senckenb. Naturforsch. Ges.* **28**, 1 (1971).
21. U. Zeller, in *Morphogenesis of the Mammalian Skull*, H.-J. Kuhn, U. Zeller, Eds. (Verlag Paul Parey, Hamburg and Berlin, 1987), pp. 17–50.
22. C. T. Clark, K. K. Smith, *J. Morphol.* **215**, 119 (1993).
23. H.-J. Kuhn, in (*21*), pp. 1–12.
24. M. R. Sánchez-Villagra, K. K. Smith, *J. Mamm. Evol.* **4**, 119 (1997).
25. P. P. Gambaryan, Z. Kielan-Jaworowska, *Acta Palaeontol. Pol.* **40**, 45 (1995).
26. R. Owen, *Monograph of the Fossil Mammalia of the Mesozoic Formations* (Paleontographical Society, London, 1871).
27. G. G. Simpson, *A Catalogue of the Mesozoic Mammalia in the Geological Department of the British Museum* (Clowes & Sons, London and Beccles, 1928).
28. A. W. Crompton, Z.-x. Luo, in (*8*), pp. 30–44.
29. A. W. Crompton, A.-l. Sun, *Zool. J. Linn. Soc.* **85**, 99 (1985).
30. K. A. Kermack, F. Mussett, H. W. Rigney, *Zool. J. Linn. Soc.* **71**, 1 (1981).
31. Z.-x. Luo, A. W. Crompton, *J. Vertebr. Paleontol.* **14**, 341 (1994).
32. A. W. Crompton, *Proc. Zool. Soc. London* **140**, 697 (1963).
33. H. R. Barghusen, J. A. Hopson, *Science N.Y.* **168**, 573 (1970).
34. Supplementary material is available at www.sciencemag.org/cgi/content/full/294/5541/357/DC1
35. We thank J. Li and Y. Wang for valuable discussion; M. Zhang, Z. Zhou, X. Xu, X. Wang, F. Zhang, F. Jin, and J. Zhang for help in coordinating the research and fieldwork; S. Xie, H. Wang (IVPP), and A. Davidson (AMNH) for preparation of the specimens; and four anonymous reviewers for instructive comments. This work is supported by the Ministry of Science and Technology, P. R. China (Major Basic Research Project, G2000077700), National Natural Science Foundation of China (49832002), and Chinese Academy of Sciences (Grand Research Projects, KZCX3-J-03, KZ951-B1-410).

27 June 2001; accepted 30 August 2001

# Genetic Basis for Activity Differences Between Vancomycin and Glycolipid Derivatives of Vancomycin

**Ulrike S. Eggert,[1] Natividad Ruiz,[2] Brian V. Falcone,[1] Arthur A. Branstrom,[3] Robert C. Goldman,[3] Thomas J. Silhavy,[2] Daniel Kahne[1]***

**Small molecules that affect specific protein functions can be valuable tools for dissecting complex cellular processes. Peptidoglycan synthesis and degradation is a process in bacteria that involves multiple enzymes under strict temporal and spatial regulation. We used a set of small molecules that inhibit the transglycosylation step of peptidoglycan synthesis to discover genes that help to regulate this process. We identified a gene responsible for the susceptibility of *Escherichia coli* cells to killing by glycolipid derivatives of vancomycin, thus establishing a genetic basis for activity differences between these compounds and vancomycin.**

Vancomycin (Fig. 1A) is the drug of last resort for treating resistant Gram-positive bacterial infections, and the emergence of vancomycin resistance presents a serious threat to public health. Vancomycin inhibits the maturation of the peptidoglycan layer surrounding bacterial cells by binding to D-Ala-D-Ala, a dipeptide found in peptidoglycan precursors (Fig. 1B) (*1*). Resistance to vancomycin arises when microorganisms acquire genes that lead to the substitution of D-Ala-D-Ala by D-Ala-D-Lac (*2*), which vancomycin does not bind. Remarkably, vancomycin derivatives with a hydrophobic substituent on the carbohydrate moiety are active against vancomycin-resistant strains (*3*) even though they contain the same peptide binding pocket as vancomycin. The mechanism of action of these derivatives may be fundamentally different from that of vancomycin (*4*). Unlike vancomycin, they retain activity against both vancomycin-sensitive and vancomycin-resistant strains even when the peptide binding pocket is damaged (*5*). In vitro, they block a different step of peptidoglycan synthesis than does vancomycin (*5*). In addition, they kill bacteria very rapidly, whereas vancomycin only stops growth (*6*).

Because vancomycin and its derivatives affect cells differently (i.e., produce different phenotypes), it might be possible, using a chemical genetics approach, to identify genes involved in the cellular response to these compounds. The synthesis of peptidoglycan from its disaccharide precursor involves numerous enzymes with overlapping functions that are subject to tight temporal and spatial regulation (*7*). Most of the major enzymes in peptidoglycan synthesis—the transglycosylases and transpeptidases—have been identified, but how these enzymes are regulated remains poorly understood. In developing an experimental approach to probe the cellular response to glycolipid derivatives of vancomycin, we focused on the following facts: Vancomycin blocks the transpeptidation step of peptidoglycan synthesis and kills cells slowly; glycolipid derivatives of vancomycin block the transglycosylation step of peptidoglycan synthesis (Fig. 1B) and provoke a rapid lethal response in cells (Fig. 1C). Moenomycin, another transglycosylase inhibitor, also induces a rapid lethal response in cells (*8*). Thus, inhibiting the transglycosylation step of peptidoglycan synthesis may activate a pathway that triggers rapid cell death. If so, it should be possible to identify components of this pathway by selecting for mutants that are resistant to small molecules that inhibit transglycosylation.

We initiated a search for mutants resistant to three different transglycosylase inhibitors: chlorobiphenyl vancomycin, desleucyl chlorobiphenyl vancomycin, and moenomycin (Fig. 1A). Moenomycin binds directly to key bacterial transglycosylases (*9*). Chlorobiphenyl vancomycin inhibits transglycosylation by binding to the D-Ala-D-Ala terminus of the peptidoglycan precursor lipid II and also by binding to components of the transglycosylation complex (*5*). Desleucyl chlorobiphenyl vancomycin cannot bind D-Ala-D-Ala and is proposed to inhibit transglycosylation primarily by the latter mechanism (*5*).

Mutants resistant to transglycosylase inhibitors were obtained by growing *E. coli imp* (*10*) on plates impregnated with chlorobiphenyl vancomycin, desleucyl chlorobiphenyl vancomycin, or moenomycin. Three mutants were isolated that were resistant to each of these antibiotics (BE101, BE102, and BE103; Table 1). The muta-

[1]Department of Chemistry, [2]Department of Molecular Biology, Princeton University, Princeton, NJ 08544, USA. [3]Advanced Medicine Inc., 901 Gateway Boulevard, South San Francisco, CA 94080, USA.

*To whom correspondence should be addressed. E-mail: dkahne@princeton.edu